

Defect formation in β -Al₂TiO₅ and its influence on structure stability

R. W. GRIMES*

The Royal Institution of Great Britain, 21 Albemarle Street, London W1X 4BS

J. PILLING

Department of Materials Engineering, Monash University, Clayton, Victoria 3168, Australia

Atomistic simulation calculations are used to predict the formation enthalpies of Schottky, Frenkel and anti-site defects. The latter are so easily formed that the β -Al₂TiO₅ structure is predicted to be essentially cation disordered, in agreement with experimental results. Conversely, conventional Schottky and Frenkel disorder is negligible and clusters of vacancy defects are strongly bound. This leads to a significant barrier for dissociation to Al₂O₃ and TiO₂ despite the positive calculated and observed formation enthalpy of Al₂TiO₅. The solution mechanisms of MgO and excess TiO₂ in β -Al₂TiO₅ are discussed.

1. Introduction

Ceramic composites containing aluminium titanate (β -Al₂TiO₅) have attracted much attention due to their low coefficients of thermal expansion [1–3]. This feature is due to the presence of grain-boundary micro-cracks that develop as a response to the high thermal anisotropy of the Al₂TiO₅ grains [4, 5]. Unfortunately, Al₂TiO₅ is only thermodynamically stable above 1281 °C and at lower temperatures will decompose into Al₂O₃ and TiO₂ [6]. However, it has been observed [7] that at temperatures below 900 °C, Al₂TiO₅ maintains its structural integrity even after annealing for up to 240 h. In addition, between 900 and 1281 °C, decomposition can be essentially arrested by adding small quantities of silicon or magnesium [7].

β -Al₂TiO₅ (tielite) is a member of the pseudobrookite family and as such, it was initially assumed that the titanium ions occupied four-fold sites and the aluminium ions eight-fold sites [8, 9]. However, as suggested by Morosin and Lynch [4] and more recently confirmed by Epicier *et al.* [10], this material exhibits a very high degree of cation disorder. The present study uses atomistic computer simulation techniques to investigate the energetics of defect formation. This includes Frenkel, Schottky and anti-site disorder and mechanisms by which MgO can be incorporated into the lattice.

2. Methodology

2.1. Simulation technique

The procedures are based upon a description of the lattice in terms of effective potentials. The perfect lattice is described by defining a unit cell which is repeated throughout space using periodic boundary conditions as defined by the usual crystallographic

lattice vectors. We consider interactions due to long-range Coulombic forces, which are summed using Ewald's method and also short-range forces that are modelled using parameterized pair potentials (as discussed below). The short-range terms account for the electron cloud overlap and dispersion interactions which are negligible beyond a few lattice spacings. Thus, in order to reduce the computational time, the short-range interactions are set to zero beyond 1.35 nm. The total energy of the crystal is minimized by allowing the ions in the unit cell and the lattice vectors to relax to zero strain.

When calculating defect energies the afore energy minimized perfect lattice is partitioned into two regions: a spherical inner region, I, at the centre of which the defect is introduced, and an outer region, II, which extends to infinity. In Region I, interactions are calculated explicitly so that the response of the lattice to the defect is modelled by relaxing the positions of all ions to zero force using a Newton–Raphson minimization procedure. The response of Region II is treated using the Mott–Littleton approximation [11]. In this study, the calculations were performed using the CASCADE code [12].

To ensure a smooth transition between Regions I and II, we incorporate an interfacial region, IIa, in which ion displacements are determined via the Mott–Littleton approximation but in which interactions with ions in Region I are calculated by explicit summation. In the present calculations, the radii of Regions I and IIa were 0.67 and 2.22 nm, respectively. Region sizes were chosen to be large enough to ensure that no appreciable change in defect formation energy occurs if the region sizes are increased further.

Oxygen ions are treated as polarizable using the shell model [13]. In this, a massless shell of charge Y is allowed to move with respect to a massive core of

* Author to whom all correspondence should be addressed.

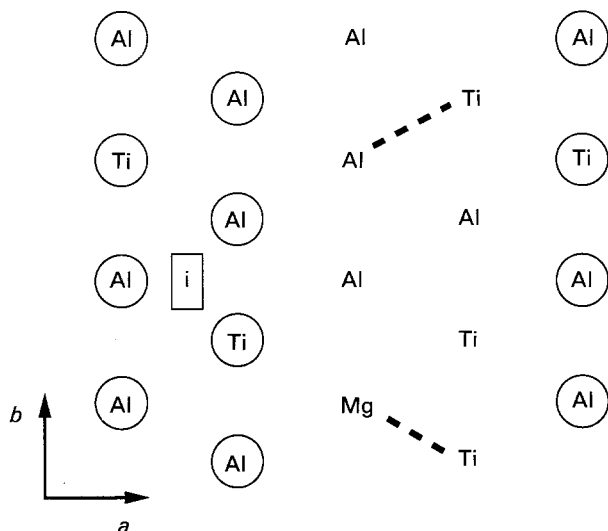


Figure 1 The ab plane showing the interstitial site i , an anti-site neutral defect pair and a neutral $\{\text{Mg}'_{\text{Al}}; \text{Ti}'_{\text{Al}}\}$ pair. Lattice ions in circles are above those not in circles by $c/2$.

charge X ; the charge state of each ion is therefore equal to $(X + Y)$. The core and shell charges are connected by an isotropic harmonic spring of force constant k (see Table I). Displacement of the shell relative to the core gives a good description of electronic polarization.

In this study, two models for ionic charges are considered. In the first model, all ions exhibit their familiar formal charges so that oxygen has a total charge of -2 . The second model relies on partial charges for all ions with oxygen now exhibiting a total charge of -1.7 . This partial charge is close to the centre of the range of values predicted by Mulliken and Löwdin population analyses of recent periodic quantum mechanical calculations of the $\alpha\text{-Al}_2\text{O}_3$ lattice [14–16]. In the absence of quantum mechanical studies of Al_2TiO_5 , Al_2O_3 is assumed to be a judicious choice of material on which to base a partial charge model pertinent to Al_2TiO_5 .

2.2. Derivation of short-range parameters

Two sets of short-range pair interactions describing the Al_2O_3 and TiO_2 perfect lattices were derived, one associated with the formal charge model, the second with the partial charge model. The Buckingham potential form was chosen to represent the interaction energy, $E(r)$, so that,

$$E(r) = A \exp(-r/\rho) - C/r^6 \quad (1)$$

where A , ρ and C are the variable parameters (see Table I). In the case of the formal charge model, the oxygen–oxygen potential was determined by simultaneously fitting the lattice parameters of a variety of oxides. As such, the range of oxygen–oxygen separations over which the potential is valid is correspondingly large, an important point when modelling lattice relaxation. The cation–anion potentials were initially determined using the approximate electron-gas method [17]. The parameters were then adjusted so that the calculated unit cell volumes of $\alpha\text{-Al}_2\text{O}_3$ and TiO_2 (rutile) were reproduced very accurately. Additional experimental data for Al_2O_3 and TiO_2 , such as elastic and dielectric constants, were also considered

TABLE I Potential parameters

	Full charge	Partial charge	
Short-range potentials			
$\text{O}^{2-}\text{-O}^{2-}$	A (eV)	9547.96	2230386.3
	ρ (nm $^{-1}$)	2.1916	1.429
	C (10^{-6} eV nm $^{-6}$)	32.0	32.0
$\text{Al}^{3+}\text{-O}^{2-}$	A (eV)	1725.2	1504.05
	ρ (nm $^{-1}$)	2.8971	2.818
$\text{Ti}^{4+}\text{-O}^{2-}$	A (eV)	2549.4	1889.4
	ρ (nm $^{-1}$)	2.989	2.989
Shell model parameters			
Oxygen shell charge (e)	-2.80	-2.23	
Oxygen total charge	-2.0	-1.7	
Oxygen harmonic constant (eV nm 2)	0.548	0.322	

in the fitting process. The same procedure was used to determine the anion–cation potential parameters associated with the partial charge model. However, the oxygen–oxygen interaction was based on the empirical potential derived by Gale *et al.* [14]. The set of potential parameters described above have also recently been used to model successfully the defect properties of alumina doped with TiO_2 , MgO and CaO [18].

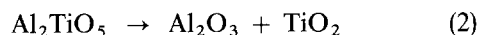
Discussions of the model parameters and of the methodology generally can be found in recent reviews [11, 19–21].

3. Results and discussion

3.1. Perfect lattice properties

In Table II the experimental crystallographic perfect lattice properties are compared to those calculated using the full and partial charge models. Both models successfully reproduce the observed orthorhombic symmetry of the unit cell. Furthermore, the unit cell volumes correlate well with the experimental value as do the a/b and a/c ratios. Finally, we note the excellent agreement with the atomic positions of the ions in the unit cell. Despite this success, we should note that Epicier *et al.* [10] claimed that their crystallographic data were relevant to a lattice which exhibited significant cation disorder. Nevertheless, the agreement increases our confidence in both potential models. Of course, the perfect lattices of Al_2O_3 and TiO_2 are also described well by both models because these formed the basis of the fitting procedure.

As mentioned in Section 1, Al_2TiO_5 disproportionates into Al_2O_3 and TiO_2 at temperatures below 1281 °C. This implies that the enthalpy for the reaction



is positive. This energy can be determined by calculating the difference in lattice energies: the values for the full and partial charge models are 0.37 and 0.56 eV, respectively. In a similar way, it is possible to calculate the increase in atomic volume for the reaction: 9.9×10^{-3} and 10.5×10^{-3} nm for the full and partial charge models, respectively. These are both in acceptable agreement, though slightly higher than the experimental value of 7.8×10^{-3} nm.

Despite the apparent structural anisotropy of the brookite lattice (Morosin and Lynch [4] describe

TABLE II Comparison of experimental perfect lattice crystallographic properties to those calculated assuming a fully cation ordered lattice

	Experimental ^a	Fully ionic model	Partially ionic model				
Lattice parameter (nm)							
<i>a</i>	0.9429	0.9591	0.9623				
<i>b</i>	0.9636	0.9878	0.9881				
<i>c</i>	0.3591	0.3530	0.3543				
Unit cell volume (nm ³)	0.3268	0.3344	0.3368				
Positional parameters							
Atom	Designation	<i>u</i>	<i>v</i>	<i>u</i>	<i>v</i>	<i>u</i>	<i>v</i>
Ti	(4c)	0.1863	0.25	0.1790	0.25	0.1792	0.25
Al	(8f)	0.1351	0.5613	0.1353	0.5597	0.1352	0.5604
O(1)	(4c)	0.759	0.25	0.764	0.25	0.765	0.25
O(2)	(8f)	0.048	0.118	0.043	0.112	0.043	0.113
O(3)	(8f)	0.317	0.075	0.299	0.075	0.299	0.075

^a See Epicier *et al.* [10]. Being experimental values, these data are relevant to a partially disordered arrangement of cations.

TABLE III Elastic and dielectric constants for the perfect, fully cation ordered lattice

	Fully ionic model	Partially ionic model
Elastic constants (10 ¹⁰ mdyn nm ⁻¹)		
<i>c</i> ₁₁	55.79	42.34
<i>c</i> ₁₂	20.56	15.02
<i>c</i> ₁₃	20.58	14.73
<i>c</i> ₂₂	48.72	38.82
<i>c</i> ₂₃	21.91	16.28
<i>c</i> ₃₃	46.99	38.01
<i>c</i> ₄₄	16.91	13.15
<i>c</i> ₅₅	5.52	3.25
<i>c</i> ₆₆	13.94	11.91
Dielectric constants		
ϵ_0		
11	5.26	4.62
22	10.68	9.07
33	6.36	5.60
ϵ_∞		
11	2.56	2.49
22	2.75	2.73
33	2.58	2.51

Al₂TiO₅ as being composed of tri-octahedral units forming infinite chains along the *c*-axis), the results in Table III suggest a fairly elastically isotropic material. This follows from the numerical similarity of *C*₁₁, *C*₂₂ and *C*₃₃ in addition to those of *C*₁₂, *C*₁₃ and *C*₂₃. It is also interesting to note that the elastic constants of this material are similar to those of Al₂O₃ (see [18]). Both models yield these results. However, given the superior correlation of the partial charge model to the experimental values for Al₂O₃, it might be expected that the same will hold true for Al₂TiO₅.

The calculated static dielectric constants suggest a much greater anisotropy although the high-frequency data are highly isotropic. Again there is a great similarity to Al₂O₃ [18] which in this case suggests that the better experimental correlation will be to the full charge model.

3.2. The defective lattice

In Table IV the calculated values, which have been

TABLE IV Calculated defect formation energies normalized per defect (eV) for fully and partially ionic models

	Isolated defects		Neutral defect clusters	
	Fully ionic	Partially ionic	Fully ionic	Partially ionic
Schottky defects				
Full	7.94	6.61		
Al partial	7.36	6.10	2.68	2.65
Ti partial	8.79	7.25	2.46	2.00
Frenkel defects				
Al Frenkel	7.19	6.10		
Ti Frenkel	11.30	7.26		
O Frenkel	5.94	4.69		
Anti-site defect	0.64	0.52	0.25	0.20

normalized per defect, for the various disorder reactions are compared. Three types of reaction are considered: Schottky, including full (leading to 5V₀^{••} + 2V_{Al}^{'''} + V_{Ti}^{'''}) and both partial reactions (i.e. 3V₀^{••} + 2V_{Al}^{'''} or 2V₀^{••} + V_{Ti}^{'''}); Frenkel (e.g. Al Frenkel where Al_i^{'''} + V_{Al}^{'''} are formed); and anti-site disorder (forming Al_{Ti}^{'''} + Ti_{Al}^{'''}). If the resulting defects are assumed to be isolated or even if defect clusters are formed (see Fig. 1), it is clear that the anti-site disorder is dramatically more favoured than any of the Schottky or Frenkel reactions.

In fact, the isolated Schottky and Frenkel reaction energies are very high, even greater than those calculated for Al₂O₃ [18] where, for example, the full charge model Schottky energy is 5.86 eV. Because we know that in Al₂O₃ the extent of Schottky and indeed Frenkel disorder is very low [18] this infers that the same will be true for Al₂TiO₅ to an even greater extent. However, Table IV also suggests that if the vacancy defects are allowed to cluster, their formation energies are much lower. The difference in the formation energies before and after defect clustering has occurred is the normalized binding energy. These energies for the partial Schottky reactions are so high that once the defects have become bound, they will remain trapped even at high temperatures.

The high values predicted for the Schottky and Frenkel reactions and the strong association of any vacancy defects that do form have important ramifications for transport phenomena. If mass transport occurs via isolated vacancy or interstitial mechanisms, there will be a high energy penalty in forming the required defects. Alternatively, if defect clusters are formed, migration must occur via a concerted motion of the defect cluster. This will lead to a much reduced pre-exponential term. Thus, because dissociation of Al_2TiO_5 into Al_2O_3 and TiO_2 requires transport of material through the lattice, the present results suggest that despite its thermodynamic instability, Al_2TiO_5 will be kinetically reluctant to dissociate. This view is supported experimentally by the thermal stability of Al_2TiO_5 below 900°C and the slow decomposition even above this temperature [7].

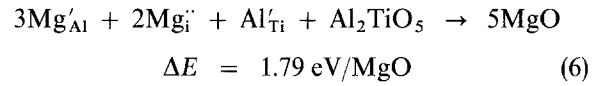
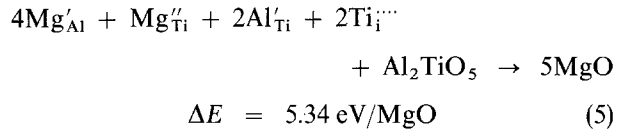
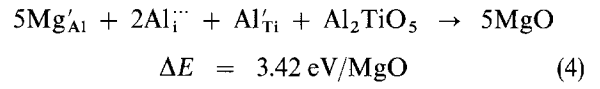
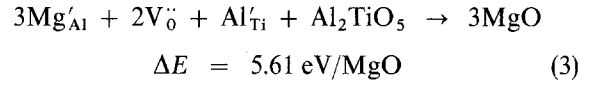
The anti-site energies were calculated assuming both isolated and clustered defects. In the case of the clustering, two nearest neighbour configurations were investigated; the first has both defects in the *ab* plane, in the second the Ti_{Al} ion and the Al_{Ti} ion are in adjacent planes. Both pairs are effectively the same distance apart (~ 0.30 nm) and return almost the same defect energy. These defect pairs therefore seem to show a fair degree of energetic isotropy.

From Bragg-Williams theory [22], for an alloy AB_2 , the total energy for disorder is $E_d = 2/18 NV_0$ where V_0 is the anti-site energy in the perfect lattice and N is the total number of sites. If we apply this to the cation sublattice of Al_2TiO_5 and normalise to one formula unit, $E_d = 0.13$ eV. The gain in configurational entropy upon randomization is $\{kT \ln W\}$ where W is the increase in the number of possible configurations that a random distribution can accommodate, k is Boltzmann's constant and T temperature. W can be calculated using the standard statistical mechanics result that $W = \{N!/(N-n)!n!\} \{M!/(M-m)!m!\}$ where, in this case N is the total number of titanium sites, n the number of aluminium ions on titanium sites, M the total number of aluminium sites and m the number of titanium ions on aluminium sites. The resulting expression is, $1.645 \times 10^{-4} T$ per Al_2TiO_5 formula unit. Thus at 1281°C , the formation temperature of Al_2TiO_5 , the sum of the configurational and Bragg-Williams disorder contributions to the free energy of formation of Al_2TiO_5 is -0.13 eV. The present calculations are, therefore, in agreement with the experimental observation that Al_2TiO_5 is cation disordered. Indeed, given the approximations inherent in the above analysis, it is possible that the configurational energy provides an important, if not critical, contribution to the formation energy of Al_2TiO_5 . The other energy term that can contribute to the formation of the brookite lattice is due to change in the vibrational entropy. Although we have not calculated it here, the increase in the unit cell volume on formation of Al_2TiO_5 (see Section 3.1) implies that the vibrational entropy term will favour the formation of the brookite lattice.

3.3. Solution of MgO

A range of different mechanisms for the solution of MgO

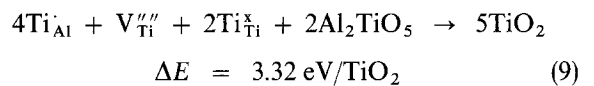
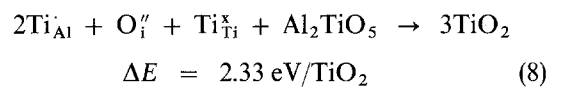
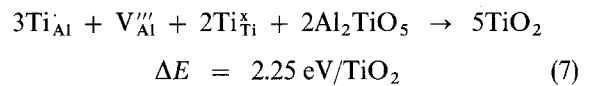
in Al_2TiO_5 were investigated. Only results from the full charge model are reported because the conclusions of both models are the same. The first three reactions assume compensation by the intrinsic oxygen vacancy or cation interstitial defects. The fourth reaction shows magnesium interstitial (Mg_i) self-compensation.



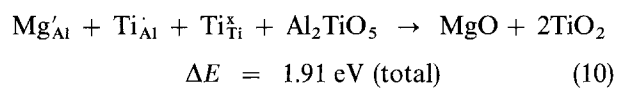
The last reaction does not require the formation of those vacancy and interstitial defects which gave rise to the exceptionally high Schottky and Frenkel energies. It is, therefore, not surprising that this self-compensating mechanism is significantly preferable. If neutral defect clusters are allowed to form, the solution energy is reduced to 0.87 eV/MgO.

3.4. Solution of excess TiO_2

If TiO_2 is present in excess of that required to form stoichiometric Al_2TiO_5 , it can be incorporated into the lattice on aluminium sites with compensation by either aluminium vacancies (Reaction 7), oxygen interstitials (Reaction 8) or titanium vacancies (Reaction 9). The calculations suggest that aluminium vacancy and oxygen interstitial compensation are preferred over titanium vacancy compensation. However, the energy difference between the aluminium vacancy and oxygen interstitial mechanisms is too small for the present method to discern between them. Rather it can be suggested that there will be strong competition between the two compensation modes.



Lastly, we have investigated the co-solution of MgO and TiO_2 . This allows for the possibility that the Mg'_{Al} and Ti_{Al} defects will self compensate so that



If clusters are allowed to form (see Fig. 1) in this case, the solution energy is reduced to 1.53 eV total. Clearly self-compensation is preferred; the total gain in energy over equivalent solution of MgO and TiO_2 is 4.38 eV (assuming isolated defects).

4. Conclusion

The behaviour of defects in Al_2TiO_5 has been investigated using atomistic computer simulation techniques. The calculations return the formation energies of isolated defects or defect clusters which are used to predict the preference of this pseudo-brookite for specific defect mechanisms. On this basis and through comparison to experiment, it transpires that although the material is particularly reluctant to form Schottky or Frenkel defects, the transposition of aluminium with titanium ions is remarkably easy.

Solution of TiO_2 and/or MgO is known to have a marked influence on the thermal stability of Al_2TiO_5 and alloys of ZrO_2 and Al_2TiO_5 . The preferred compensation mechanisms which allow magnesium and titanium ions to occupy lattice or interstitial sites were therefore studied. In the case of MgO solution, self-compensation by magnesium interstitial ions is favoured. For TiO_2 solution, compensation by either oxygen interstitials or aluminium vacancies is energetically similar. Much more preferable, however, is co-solution of both MgO and TiO_2 because magnesium and titanium ions substituted on aluminium sites are charge self-compensating.

Acknowledgement

This work was supported in part by a grant from Caterpillar Inc.

References

1. H. MORISHIMA, Z. KATO, K. UEMATSU, K. SAITO, T. YANO and N. OOTSUKA, *J. Am. Ceram. Soc.* **69** (1986) C-226.
2. F. J. PARKER, *ibid.* **73** (1990) 929.

3. P. VIRRO-NIC and J. PILLING, *J. Mater. Sci. Lett.* submitted.
4. B. MOROSIN and R. W. LYNCH, *Acta Crystallogr.* **B28** (1972) 1040.
5. Y. OHYA, Z. NAKAGAWA and K. HAMANO, *J. Am. Ceram. Soc.* **70** (1987) C-184.
6. E. KATO, K. DAIMON and J. TAKAHASI, *ibid.* **63** (1980) 355.
7. M. ISHITUKA, T. SATO, T. ENDO and M. SHIMADA, *ibid.* **70** (1987) 69.
8. A. E. AUSTIN and C. M. SCHWARTZ, *Acta Crystallogr.* **6** (1953) 812.
9. M. HAMELIN, *Bull. Soc. Chim. 5^e série* (1958) 1559.
10. T. EPICIER, G. THOMAS, H. WOLFROMM and J. S. MOYA, *J. Mater. Res.* **6** (1991) 138.
11. C. R. A. CATLOW and W. C. MACKRODT, in "Computer Simulation of Solids", edited by C. R. A. Catlow and W. C. Mackrodt (Springer-Verlag, Berlin, 1982) pp 3-20.
12. M. LESLIE, SERC Daresbury Laboratory Report DL/SCI/TM31T (1982).
13. B. G. DICK and A. W. OVERHAUSER, *Phys. Rev.* **112** (1958) 90.
14. J. D. GALE, C. R. A. CATLOW and W. C. MACKRODT, *Modelling Simul. Mater. Sci. Eng.* **1** (1992) 73.
15. D. E. ELLIS, J. GUO and D. L. LAM, *Rev. Solid State Sci.* **5** (1991) 287.
16. P. W. M. JACOBS and E. A. KOTOMIN, *Phys. Rev. Lett.* **69** (1992) 1411.
17. J. H. HARDING and A. H. HARKER, UKAEA Harwell Report R-10425. (United Kingdom Atomic Energy Authority, Harwell, UK, 1982).
18. R. W. GRIMES, *J. Am. Ceram. Soc.*, in press.
19. C. R. A. CATLOW and A. M. STONEHAM (Guest editors), special issue *J. Chem. Soc. Farad. Trans.* **85**(5) (1989).
20. A. H. HARKER and R. W. GRIMES (Guest editors), special issue *Mol. Simul.* **4**(5) (1990).
21. *Idem*, *ibid.* **5**(2) (1990).
22. F. C. NIX and W. SHOCKLEY, *Rev. Mod. Phys.* **10** (1938) 1.

Received 10 August

and accepted 14 September 1993